The role of the tunneling component in the current–voltage characteristics of metal-GaN Schottky diodes

L. S. Yu,[a] Q. Z. Liu, Q. J. Xing, D. J. Qiao, and S. S. Lau
Department of Electrical and Computer Engineering, University of California, San Diego, California 92093-0407

J. Redwing
Epitronics/ATMI, 21002 North 19 Avenue, Suite 5, Phoenix, Arizona 85022

(Received 26 March 1998; accepted for publication 5 May 1998)

The temperature dependence of the current–voltage characteristics of Ni–GaN Schottky barriers have been measured and analyzed. It was found that the enhanced tunneling component in the transport current of metal-GaN Schottky barrier contacts is a likely explanation for the large scatter in the measured Richardson constant. © *1998 American Institute of Physics.* [S0021-8979(98)01316-4]

I. INTRODUCTION

The study of Schottky barrier contacts on GaN has great importance for high temperature, high frequency, and high power devices. In recent years, substantial effort has been focused on the investigation of electrical properties of metal-GaN Schottky diodes. Electrical characteristics [current–voltage ($I-V$) and capacitance–voltage ($C-V$)] of Schottky barriers of Au, Pt, Pd, Ti, and Ni on *n*-GaN have been reported in the literature.[1–6]

In general, the $I-V$ characteristics of a Schottky diode can be described by

$$I=I_s\left(\exp\left(\frac{qV}{nkT}\right)-1\right), \quad I_s=A_eA^*T^2\exp\left(\frac{-q\phi_b}{kT}\right), \tag{1}$$

where A^*=Richardson constant, k=Boltzmann constant, A_e=area of diode, $q\phi_b$=Schottky barrier height, n=ideality factor, and V=applied voltage. From the temperature dependence of the $I-V$ characteristics (the $I-V-T$ characteristics), a Richardson plot of $\ln[I_s/(A_eT^2)]$ vs $1/T$ can be obtained. According to Eq. (1), the plot should be a straight line and the barrier height and the Richardson constant, A^*, can be determined independently. $C-V$ measurements can be used to obtain the donor concentration and the barrier height.[7]

We have previously studied a variety of metals contacts to *n*-GaN, such as Pt, Pd, PtSi, Ni, and NiSi[8–10] and have determined that the $I-V$ characteristics were strongly dependent on the GaN material quality. From reported results[1–6] and our experimental results, it was noted that there is a large scattering in the measured value of the Richardson constant. Values of A^* of 0.006[1] and 14.68[3] A cm^{-2} K^{-2} for Au, 0.04,[5] 0.44,[6] and 3.2[4] A cm^{-2} K^{-2} for Pd, 6.61[6] and 64.7[4] A cm^{-2} K^{-2} for Pt have been reported. Almost all published values of A^* are far from the theoretical Richardson constant of GaN (26 A cm^{-2} K^{-2}).[2] It should be noted that the barrier heights measured by the $I-V-T$ method are usually 0.1 eV smaller than those obtained by $C-V$ measurements. The difference cannot be completely accounted for by the image force lowering.[7] According to Hacke and others,[1–3] the small value of A^* and the difference in $q\phi_b$ values measured by $I-V$ and $C-V$ may be attributable to the presence of a very thin interfacial layer between the metal and GaN.

In this work we studied the carrier transport mechanisms of GaN Schottky barriers and found that the enhanced tunneling component in the transport current is a likely explanation for the large scatter in the measured Richardson constant as well as the discrepancy between ($I-V-T$) and $C-V$ barrier height values.

II. THEORETICAL ANALYSIS

Figure 1 shows the energy band diagram for a metal semiconductor contact under forward bias. Electrons from the semiconductor conduction band can be transported to the metal by two mechanisms. They can overcome the barrier by having energy larger than the maximum effective barrier height, or can tunnel through it. The current density $J_{s\to m}$ from the semiconductor to the metal is given by[7]

$$J_{s\to m}=\frac{A^*T}{k}\int_0^{\infty}T(\zeta)\exp\left(\frac{-q(V_{b0}+V_n+\zeta-\Delta\phi)}{kT}\right)d\zeta + \frac{A^*T}{k}\int_0^{q(V_{b0}-\Delta\phi)}F_sT(\eta)(1-F_m)d\eta, \tag{2}$$

where F_s=Fermi–Dirac distribution function in the semiconductor, F_m=Fermi–Dirac distribution function in the metal, $q\phi_{b0}$=the barrier height of the metal-semiconductor contact, ignoring the image force lowering, $q\Delta\phi$=the image force lowering of the barrier height (see Fig. 1). We define the effective barrier height here as $q\phi_b=q\phi_{b0}-q\Delta\phi$ and the effective flat band voltage as $qV_b=qV_{b0}-q\Delta\phi$, $T(\xi)$=the quantum transmission coefficient of the electrons over the effective barrier, $T(\eta)$=the quantum transmission coefficient of the electrons below the top of the effective barrier, ξ=the energy of the electrons above the top of the effective barrier, η=the energy of the electrons below the top of the

[a]Electronic mail: lsyu@celece.ucsd.edu

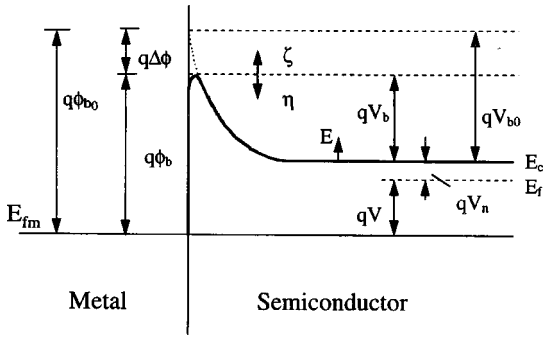

FIG. 1. Schematic band diagram of a metal-semiconductor contact under forward bias, where E_f = quasi-Fermi level of semiconductor, E_{fm} = Fermi level of metal, E_c = bottom of the conduction band of semiconductor, ζ = energy of the electrons above the top of the effective barrier, η = energy of the electrons below the top of the effective barrier, E = energy of electrons measured from the bottom of the conduction band, V = applied voltage, $qV_n = E_c - E_F$, $q\phi_{b0}$ = barrier height of the metal-semiconductor contact ignoring image force lowering, $q\Delta\phi$ = image force lowering of the barrier height. The effective barrier height is defined here as $q\phi_b = q\phi_{b0} - q\Delta\phi$ and the effective flat band voltage as $qV_b = qV_{b0} - q\Delta\phi$.

effective barrier, E = the energy of the electrons measured from the bottom of conduction band, qV_n = Fermi level measured as $E_c - E_F$. From Fig. 1, we have

$$\eta = qV_b - E, \tag{3}$$

and under forward bias

$$qV_b = q\phi_b - qV_n - qV. \tag{4}$$

Under forward bias Eq. (2) can be written as

$$J_{s\to m} = \frac{A^*T}{k}\int_0^{\infty} T(\zeta)\exp\left(\frac{-q(V_b+V_n)}{kT}\right)\exp\left(-\frac{\zeta}{kT}\right)d\zeta + \frac{A^*T}{k}\int_0^{qV_b} F_s T(\eta)(1-F_m)\,d\eta = A + B. \tag{5}$$

Using Eq. (4) and assuming $T(\zeta)=1$, the first term of Eq. (5), A, becomes

$$A = A^*T^2\exp\left(\frac{-q\phi_b}{kT}\right)\exp\left(\frac{qV}{kT}\right). \tag{6}$$

This gives the typical thermionic current. The second term of Eq. (5), B, is due to the tunneling component. Under forward bias, in the metal side, we only concern the occupation of energy levels above the Fermi level, so we can assume $F_m = 0$. Then, for a nondegenerate semiconductor, F_s is given by

$$F_s = \exp\left(\frac{-qV_n}{kT}\right)\exp\left(\frac{-E}{kT}\right). \tag{7}$$

Assuming the barrier has a triangular shape, the tunneling probability for electrons at the bottom of the conduction band is[11]

$$T(V_b) = \exp\left(-\frac{4}{3}\frac{\sqrt{2m^*}}{\hbar}\sqrt{qV_b}d\right),$$

where m^* = the effective mass of the electrons in semiconductor, $\hbar$ = Plank's constant divided by 2π, d is the width of the barrier at the base,

$$d = \sqrt{\frac{2\epsilon_s}{qN_d}}\sqrt{V_b},$$

therefore,

$$T(V_b) = \exp\left(-\frac{8}{3}\sqrt{\frac{m^*\epsilon_s}{N_d}}\frac{1}{\hbar}V_b\right) = \exp\left(\frac{-qV_b}{E_{00}}\right), \tag{8a}$$

and

$$E_{00} = \left(\frac{8}{3}\sqrt{\frac{m^*\epsilon_s}{N_d}}\frac{1}{q\hbar}\right)^{-1}, \tag{8b}$$

where ϵ_s = the semiconductor dielectric constant, and N_d = semiconductor doping concentration. The second term of Eq. (5) becomes

$$B = \frac{A^*T}{k}\int_0^{qV_b}\exp\left(\frac{-qV_n}{kT}\right)\exp\left(\frac{-E}{kT}\right)T(\eta)\,d\eta. \tag{9}$$

Since the electrons have an exponential distribution with E, most of the contribution comes from the electrons at the bottom of the conduction band (where E is small), so the tunneling probability inside the integral can be approximated by Eqs. (3) and (8)[7] to be

$$T(\eta) \sim \exp\left(\frac{-\eta}{E_{00}}\right). \tag{10}$$

Combining Eqs. (3), (4), and (10), Eq. (9) can be written as

$$\begin{aligned} B &= \frac{A^*T}{k}\int_0^{qV_b}\exp\left(-\frac{(q\phi_b - qV)}{kT}\right) \times\exp\left(\frac{\eta}{kT}\right)\exp\left(\frac{-\eta}{E_{00}}\right)d\eta \\ &= \frac{A^*T^2}{\alpha}\left(\exp\left(\frac{-q\phi_b}{kT}\right)\exp\left(\frac{qV}{kT}\right) - \exp\left(\frac{-q\phi_b}{E_{00}}\right) \times\exp\left(\frac{qV}{E_{00}}\right)\exp\left(\alpha\frac{qV_n}{kT}\right)\right), \end{aligned} \tag{11}$$

where $\alpha = [(kT/E_{00}) - 1]$. Therefore, the total current from semiconductor to metal is

$$\begin{aligned} I_{s\to m} &= A_e A^*T^2\exp\left(\frac{-q\phi_b}{kT}\right)\exp\left(\frac{qV}{kT}\right) \\ &\quad + \frac{A_e A^*T^2}{\alpha}\left(\exp\left(\frac{-q\phi_b}{kT}\right)\exp\left(\frac{qV}{kT}\right)\right. \\ &\quad \left. - \exp\left(\frac{-q\phi_b}{E_{00}}\right)\exp\left(\frac{qV}{E_{00}}\right)\exp\left(\alpha\frac{qV_n}{kT}\right)\right). \end{aligned} \tag{12}$$

When $E_{00}\to 0$, the second term of Eq. (12) becomes zero and Eq. (12) reduces to Eq. (1) with $n=1$, as a pure thermionic current.

From Eq. (8) the tunneling probability is dependent on the doping concentration N_d in GaN. For $N_d = 1\times10^{17}/\text{cm}^3$, $E_{00} = 0.00313$ eV; for $N_d = 5\times10^{17}/\text{cm}^3$, $E_{00} = 0.0112$

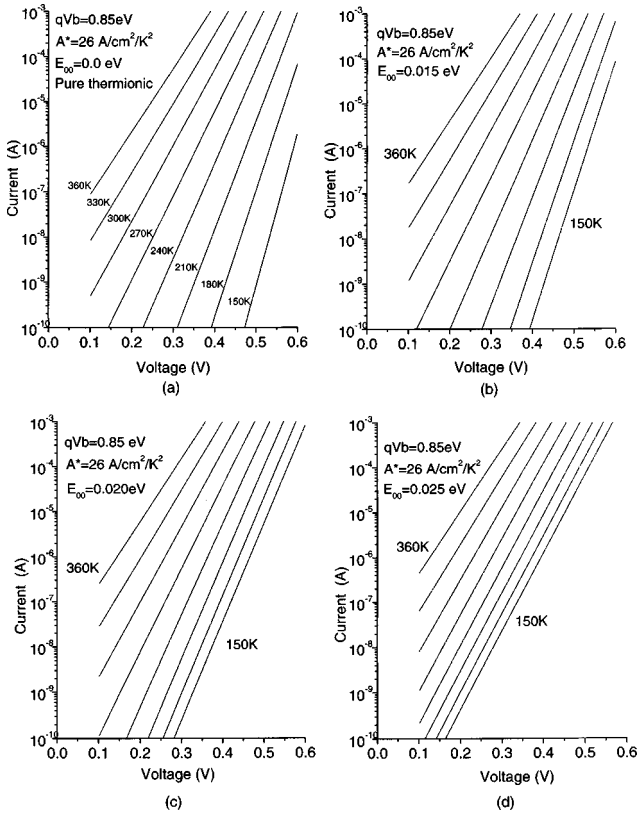

FIG. 2. Calculated $I-V-T$ characteristics in the temperature range of 150–360 K using Eq. (12) with an assumed effective barrier height, $q\phi_b$, of 0.85 eV, effective Richardson constant $A^*=26\ \mathrm{A\ cm^{-2}\ K^{-2}}$, Schottky contact area $A_e=8.04\times10^{-4}\ \mathrm{cm^2}$ and (a) $E_{00}=0.0$, (b) $E_{00}=0.015$, (c) $E_{00}=0.020$, and (d) $E_{00}=0.025$ eV. The effects of series resistance have not been included in the calculation.

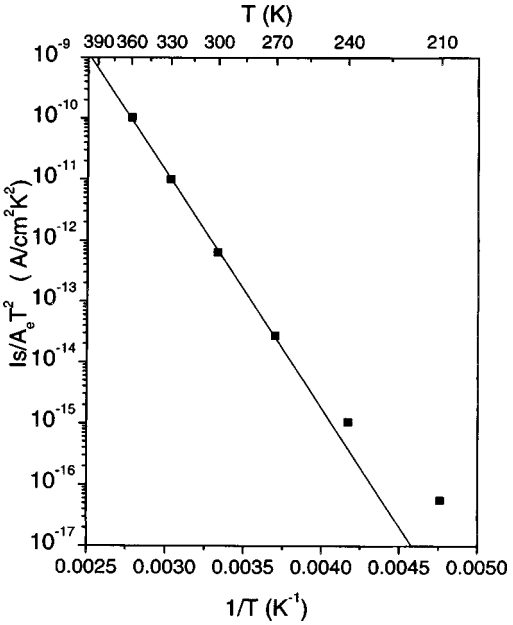

FIG. 3. Richardson plot of I_s/A_eT^2 vs $1/T$, using Eq. (1) and the calculated results in Fig. 2(c) where $E_{00}=0.020$ eV. The solid square symbol (■) is the calculated value for each temperature. The plot [represented by (■) symbols] does not appear to be linear over the entire temperature range of investigation, however, in the temperature range between 270 and 360 K the data fit a straight line quite well. A barrier height of 0.77 eV and an effective Richardson constant, A^*, of $5.92\ \mathrm{A\ cm^{-2}\ K^{-2}}$ can be obtained from this straight line.

eV and for $N_d=1\times10^{18}/\mathrm{cm^3}$, $E_{00}=0.0178$ eV. Usually in the case of $N_d=1\times10^{17}/\mathrm{cm^3}$, E_{00} is quite small and the contribution from tunneling is negligible. It is well known that GaN usually has a high dislocation density, much more than those in Si and GaAs. If there were many defects near the surface region, electrons can go through the barrier by defect-assisted tunneling, thus greatly enhancing the tunneling probability. The details of this kind of tunneling process are not known. However, we can still analyze the phenomenon by redefining the parameter E_{00} to describe the effect of defect-assisted tunneling. Equation (12) obtained above may still be used by assuming a value of E_{00} which is larger than the value obtained from Eq. (8b), i.e., from the doping concentration alone.

Theoretically calculated forward $I-V-T$ curves using Eq. (12) for $V>3kT/q$ are shown in Figs. 2(a)–2(d). The following parameters were used in the calculation: $A^*=26\ \mathrm{A\ cm^{-2}\ K^{-2}}$, $q\phi_b=0.85$ eV and the Schottky barrier area $A_e=8.04\times10^{-4}\ \mathrm{cm^2}$ (the actual diode area used in our experiments). The series resistance has not been taken into consideration. For intermediate and high temperature regions, the donors are expected to be fully ionized and the Fermi level is given by

$$qV_n=E_c-E_F=-kT\ \ln\frac{N_d}{N_c}, \tag{13}$$

where N_c is the effective density of states in the conduction band of GaN.

The doping concentration of the samples used in our experiments was determined by $C-V$ measurement. It is about $N_d=1\times10^{17}/\mathrm{cm^3}$. Therefore, E_{00} should be 0.00313 eV according to Eq. (8).

To see the effects of E_{00} on the $I-V-T$ characteristics, four different values of E_{00} (0.0, 0.015, 0.020, and 0.025 eV) have been assumed in our calculation. It can be seen from Fig. 2 that as E_{00} increases, the $I-V-T$ curves change due to the increasing contribution of the tunneling component. For small values of E_{00} (0.0 and 0.015 eV), the slope of the $I-V$ curve changes as temperature changes [Figs. 2(a) and 2(b)]. For larger values of E_{00} (0.020 and 0.025 eV), the $I-V$ curves are more closely spaced, and the log I vs V curves in the low temperature regime are almost parallel. At high temperatures, the slope of the $I-V$ curves still changes slightly as the temperature changes, indicating that the thermionic current is increasing more significant at higher temperatures [Figs. 2(c) and 2(d)].

In using the Richardson plot to obtain $q\phi_B$ and A^*, the current transport mechanism must be primarily due to thermionic emission. If this was not the case, the Richardson plot would yield erroneous results. For example, using the calculated results shown in Fig. 2(c) ($E_{00}=0.020$ eV) and Eq. (1), $I_s/(A_eT^2)$ was plotted against $1/T$ in the temperature range 210–360 K as shown in Fig. 3. The plot does not appear linear. However, in the temperature range of 270–360 K, the results can be described by a straight line reasonably well (solid line in Fig. 3). Since most of the published data of the barrier height and the Richardson constant were obtained

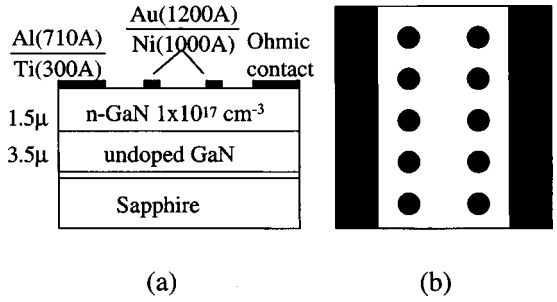

FIG. 4. Schematics of the sample structure. (a) Cross-sectional view, (b) top view.

from experimental $I-V-T$ curves in this temperature range,[1,3–6] we used the data within this temperature range to deduce a barrier height, $q\phi_b$, of 0.77 eV and a A^* value of 5.92 A cm^{-2} K^{-2} from the linear fit. It can be seen that both the barrier height and the Richardson constant are quite different from the initially assumed values for the calculation of $q\phi_b=0.85$ eV and $A^*=26$ A cm^{-2} K^{-2}. This observation indicates that a linear Richardson plot does not necessarily give the correct values of $q\phi_b$ and A^*. Furthermore, the thermionic transport mechanism requires that the n factor be a constant for different temperatures and close to 1.0, however, we found from Fig. 2(c) that $n=1.02$ for 300 K, $n=1.05$ for 240 K, $n=1.13$ for 210 K, and $n=1.29$ for 180 K, indicating that a deviation from thermionic emission at decreasing temperature for a case where $E_{00}=0.020$ eV.

In principle, recombination current may also contribute to the carrier transport. The recombination current is due to the minority carrier injection in the Schottky barrier region. Usually in the wide band gap semiconductor minority carrier injection is small, therefore, the recombination current should be insignificant. The ratio of the thermionic to recombination current can be estimated by[12]

$$T^2\tau\exp\{q(E_g+V-2\phi_b)/2kT\}, \tag{14}$$

where τ is the lifetime of the carriers and is usually larger than 10^{-10} s,[13] E_g is the energy band gap of the GaN and is about 3.42 eV, therefore, the recombination current in our case is negligible. For this reason we only considered the thermionic and tunneling current in our analysis.

III. EXPERIMENTAL PROCEDURE

The GaN substrates were grown in a metal organic vapor phase epitaxy (MOVPE) system. The details of the growth process have been reported elsewhere.[14] The structure of the samples consists of a 1.5-μm-thick n-type ($\sim1\times10^{17}$ cm^{-3}) GaN layer on top of a 3.5-μm-thick undoped GaN layer that has a high resistivity on a sapphire (0001) substrate. The sample structure and diode configuration are shown in Figs. 4(a) and 4(b), respectively. Schottky barriers were prepared as follows: GaN substrates were first cleaned by trichloroethylene, acetone, and two-propanol sequentially. Using liftoff techniques, a bilayer structure Al(710 Å)/Ti(300 Å) in the shape of strips were e-beam deposited on GaN as ohmic contacts in a vacuum of 1×10^{-7} Torr. Before loading into the vacuum chamber, the patterned samples were etched in a HF:HCl:H_2O=1:1:2 solution for about 7 to 8 s as a final cleaning step. Low-resistance ohmic contacts were obtained after rapid thermal annealing (RTA) at 600° C for 40 s in a flowing N_2 ambient. Using a similar procedure, 1000 Å of Ni followed by 1200 Å of Au was deposited on GaN for the Schottky barrier contact. The diameter of the diode was 320 μm. The gold layer was only for wire bonding purposes for low temperature measurements.

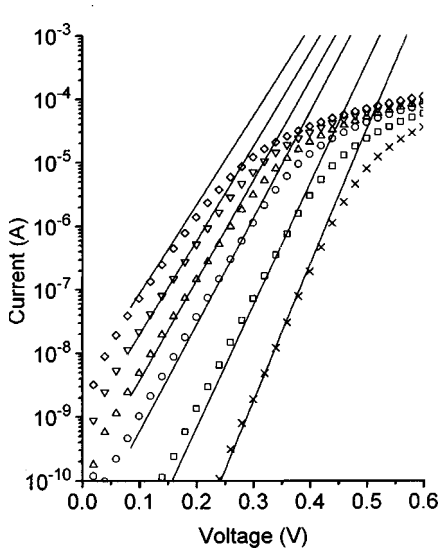

FIG. 5. Experimental $I-V-T$ curves of Ni–GaN (n type) Schottky barriers. Discrete dots are experimental results ($\diamond=360$, $\triangledown=340$, $\triangle=320$, $\bigcirc=300$, $\square=260$, and $\times=220$ K). Solid lines are the simulated curves using Eq. (12) with assumed values of $q\phi_b=0.88$ eV, $A^*=26$ A cm^{-2} K^{-2} and $E_{00}=0.0195$ eV. The simulated curves can represent the experimental results reasonably well. The bending of experimental curves in high voltage regime is caused by the series resistance which has not been included in the simulation.

IV. EXPERIMENTAL RESULTS AND DISCUSSION

Current–voltage characteristics of Ni–GaN (n-type) Schottky diodes as a function of temperature (220–360 K), and capacitance–voltage ($C-V$) characteristics at room temperature were measured in this investigation. Figure 5 shows the typical $I-V-T$ characteristics obtained on the diodes. The experimental points are represented by various symbols in the figure. The theoretical $I-V-T$ curves [Eq. (12)] with $q\phi_b=0.88$ eV, $A^*=26$ A cm^{-2} K^{-2}, and $E_{00}=0.0195$ eV are also shown as solid lines in Fig. 5. The series resistance (~1.5 kΩ) was not included in the calculation. The theoretical curves appear to describe the experimental results reasonably well. Since the experimental results can be described by the thermionic current transport model, we proceeded to extract the barrier height and A^* from the experimental results shown in Fig. 5 using the Richardson plot. Figure 6 shows the Richardson plot, and we can see that all six datum points fall on a straight line (the solid line) reasonably well. Using this solid line shown in Fig. 6, a barrier height $q\phi_b=0.61$ eV and $A^*=0.0079$ A cm^{-2} K^{-2} were obtained. However, upon closer inspection of Fig. 6, we noted that the four datum points for temperatures higher than 300 K could be fitted to a straight line better (the dashed line).

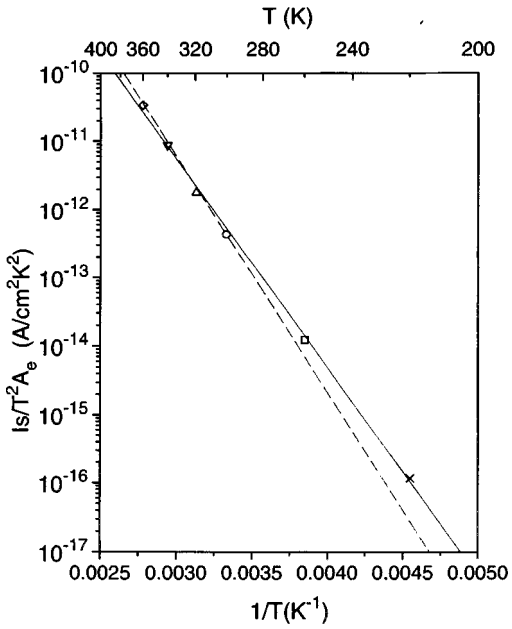

FIG. 6. Richardson plot of I_s/A_eT^2 vs $1/T$ using Eq. (1) and the experimental results shown in Fig. 5. A barrier height of 0.61 eV and an effective Richardson constant $A^*=0.0079$ A cm^{-2} K^{-2} were obtained by fitting the all datum points to a straight line (solid line). For a more accurate fitting a barrier height of 0.69 eV and $A^*=0.129$ A cm^{-2} K^{-2} were obtained in the temperature range 300–360 K (dash line). In this temperature regime, thermionic emission current is more significant, leading to larger values of barrier height and Richardson constant.

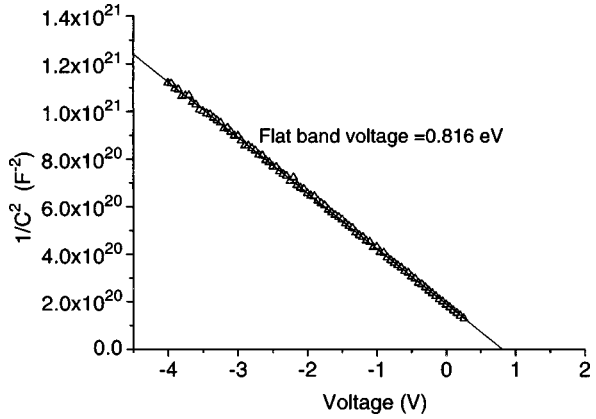

FIG. 7. Experimental $1/C^2$ vs V relationship at room temperature for the same diode shown in Fig. 5. The frequency used in the measurement is 20 kHz. The deduced Schottky barrier height is 0.92 eV with a carrier concentration of 1×10^{17} cm^{-3}.

From the dashed line, a barrier height of 0.69 eV and $A^*=0.129$ A cm^{-2}K^{-2} can be deduced. The datum points at lower temperatures (260 and 220 K) were off the dashed line, very similar to what was shown in Fig. 3. These results suggest that the transport mechanism became more thermionic at higher temperatures. The values of the Richardson constant obtained from the solid and the dashed line are far from the theoretical value $A^*=26$ A cm^{-2} K^{-2}, which was the value used in the calculation shown as straight lines in Fig. 5.

The results of the $C-V$ measurements at room temperature for this sample is shown in Fig. 7. A doping concentration of $\sim1\times10^{17}$ cm^{-3} and a Schottky barrier height of $\sim$0.92 eV were obtained from $1/C^2-V$ relationship. The barrier height obtained from $C-V$ measurements, $\phi(C-V)$, is the barrier height at zero electric field (or flat band), and can be considered to be $q\phi_{b0}$ (Fig. 1), which does not include image force lowering. This barrier height is usually larger than the barrier height, $q\phi_b$, determined from $I-V$ measurements. Since the estimated image force lowering in the Ni/GaN case is about 0.045 eV, it appears that the simulated $\phi(I-V)$ of 0.88 eV shown in Fig. 5, which is slightly lower than 0.92 eV [$\phi(C-V)$], was in reasonable agreement (note that the simulation assumed $E_{00}=0.0195$ eV). The barrier height obtained from $I-V-T$ measurements shown in Fig. 6 yielded a $\phi(I-V)$ value of 0.61–0.69 eV, 0.2–0.3 eV smaller than that determined from the $C-V$ measurements. This large discrepancy cannot be explained by the image force lowering alone. Hacke and *et al.*[1–3] rationalized a similarly large discrepancy in barrier heights between $C-V$ and $I-V$ measurements and the large difference between the theoretical and experimental values of A^* by the presence of a interfacial layer between the metal and GaN surface. Since we have shown previously[9,10] that metal layers such as Ni can be deposited epitaxially on GaN surfaces etched in a HF:HCl:H_2O solution, the possibility of the presence of an interfacial layer may not be too prominent. On the other hand, the epitaxial nature of the as-deposited Ni film does not preclude the possibility of a nonuniform interfacial layer. In this case, the $I-V$ characteristics will show more complicated behavior. The model presented here may not depict the actual physical situation. However, the thermionic mechanism predicts a constant ideality factor, n (n can be larger than 1), for different temperatures regardless of the presence of an interfacial layer,[15] but, our experimental results show increasing n factor values with decreasing temperature ($n=1.06$ for 340 K, $n=1.10$ for 300 K, $n=1.22$ for 220 K, see Fig. 5), in contrast to the interfacial layer model. The experimental observation of an increasing n with decreasing temperatures and other experimental facts are consistent with the notion that tunneling plays an important role in the transport of carriers across the Schottky barrier on n-GaN, even for doping concentrations as low as 1×10^{17} cm^{-3}. The enhanced role of the tunneling component is probably induced by the large amount of defects in GaN.

It is well established that the crystal quality of Si and GaAs are far superior than that of GaN. For Schottky barriers on Si and GaAs with a doping concentration of 10^{16} cm^{-3}, tunneling does not play a role in the transport mechanism. For Si, it has been reported that the n factor for Schottky diodes on Si was 1.02 and remained constant in the temperature range of 100–300 K;[16] the experimental value of A^* was found to be 90 A cm^{-2} K^{-2} in reasonable agreement with the theoretical value of 112 A cm^{-2} K^{-2}. For GaAs, the experimental value of A^* has been reported to be 11 A cm^{-2} K^{-2},[17,18] also in reasonable agreement with the theoretical value of 8.8 A cm^{-2} K^{-2}. These results reported in the literature showed that a meaningful Richardson constant for Si and GaAs can be readily extracted from $I-V-T$ measurements. In the present work, we have demonstrated that the

$I-V-T$ characteristics are very likely to be influenced by the tunneling current in carrier transport in nondegenerate but highly defective materials, thus making the determination of the barrier height and the Richardson constant difficult using the $I-V-T$ method.

V. SUMMARY

The carrier transport mechanisms for Ni–GaN Schottky barriers have been investigated using $I-V-T$ and $C-V$ measurements. From the theoretical analysis and experimental results, it was found that the enhanced tunneling effect for GaN Schottky barriers with defects near the surface region is a likely cause for the large scattering in the Richardson constant as measured by the $I-V-T$ method, and the large discrepancy in the barrier height between $I-V-T$ and $C-V$ measurements.

ACKNOWLEDGMENTS

The authors wish to thank Professor C. D. Wang (UCSD) for helpful discussion. The work at UCSD is supported by BMDO (Dr. Kepi Wu), monitored by the U.S. Army Space and Missile Defense Command, and by the National Science Foundation, NSF.

[1] P. Hacke, T. Detchprohm, K. Hiramatsu, and N. Sawaki, Appl. Phys. Lett. **63**, 2676 (1993).
[2] M. Khan, T. Detchprohm, P. Hacke, K. Hiramatsu, and N. Sawaki, J. Phys. D **28**, 1169 (1995).
[3] A. T. Ping, A. C. Schmitz, M. Asif Khan, and I. Adesida, Electron. Lett. **32**, 68 (1996).
[4] A. C. Schmitz, A. T. Ping, M. Asif Khan, Q. Chen, J. W. Yang, and I. Adesida, Semicond. Sci. Technol. **11**, 1464 (1996).
[5] L. Wang, M. I. Nathan, T. H. Lim, M. A. Khan, and Q. Chen, Appl. Phys. Lett. **68**, 1267 (1996).
[6] J. D. Guo, M. S. Feng, R. J. Guo, F. M. Pan, and C. Y. Chang, Appl. Phys. Lett. **67**, 2657 (1995).
[7] S. M. Sze, *Physics of Semiconductor Devices*, 2nd ed. (Wiley, New York, 1981), Chap. 5.
[8] Q. Z. Liu, L. S. Yu, S. S. Lau, J. M. Redwing, N. R. Perkins, and T. F. Kuech, Appl. Phys. Lett. **70**, 1275 (1997).
[9] Q. Z. Liu, L. Shen, K. V. Smith, C. W. Tu, E. T. Yu, S. S. Lau, N. R. Perkins, and T. F. Kuech, Appl. Phys. Lett. **70**, 990 (1997).
[10] Q. Z. Liu, L. S. Yu, S. S. Lau, J. M. Redwing, and N. R. Perkins, J. Appl. Phys. (to be published).
[11] R. A. Smith, in *Wave Mechanics of Crystalline Solids* (Chapman and Hall, London, 1961), p. 49.
[12] E. H. Rhoderick and R. H. Williams, in *Metal-Semiconductor Contacts*, 2nd ed. (Oxford Science, Oxford, 1988), p. 118.
[13] G. D. Chen, M. Smith, J. Y. Lin, H. X. Jiang, S.-H. Wei, M. Asif Khan, and C. J. Sun, Appl. Phys. Lett. **68**, 2784 (1996).
[14] J. M. Redwing, J. S. Flynn, M. A. Tischler, W. Mitchel, and A. Saxler, Mater. Res. Soc. Symp. Proc. **395**, 201 (1996).
[15] H. C. Card and E. H. Rhoderick, Solid-State Electron. **16**, 365 (1973).
[16] M. Wittmer, Phys. Rev. B **43**, 4385 (1991).
[17] F. A. Padovani and G. G. Summer, J. Appl. Phys. **36**, 3744 (1965).
[18] S. X. Jin, L. P. Wang, M. H. Yuan, J. J. Chen, Y. Q. Jia, and G. G. Qin, J. Appl. Phys. **71**, 536 (1992).